3rd URSI AT-AP-RASC, Gran Canaria, 29 May – 3 June 2022

Scattering Properties of High-Permittivity Dielectric Resonators Embedded with Impedance Sheets

Rasmus E. Jacobsen* (1), Andrei V. Lavrinenko(2), and Samel Arslanagić(3).
(1), (3) National Space Institute, Technical University of Denmark, Kongens Lyngby, 2800, Denmark,
e-mail: (1) rajac@elektro.dtu.dk, (3) sar@elektro.dtu.dk.
(2) Department of Photonics Engineering, Technical University of Denmark, Kongens Lyngby, 2800, Denmark,
e-mail: (2) alav@fotonik.dtu.dk.

Abstract

Scattering from small dielectric resonators has been of high interest in the recent years for many applications such as metasurfaces and antennas with frequency operation from microwaves to optics. Various dielectric resonators have been studied; however, recently it was shown that the same type of resonances, namely Mie resonances, can be excited in impedance sheets with reactive impedances. Presently, we study a configuration consisting of a high-permittivity infinitely long, circular cylinder embedded with a coaxial impedance sheet. We present the analytical solution for the evaluation of the scattering properties for both transverse electric and magnetic plane wave illuminations. We show that resonances are excited in both the dielectric medium and the impedance sheet, and furthermore, that these resonances can be effectively tailored by changing the size of the cylinder and impedance sheet. We report on several designs with interesting scattering properties including the simultaneous excitation of magnetic and electric resonances, i.e., a Huygens type of response. Our results are general and may serve as a guideline for interesting metamaterial and antenna designs as well as graphene nanotubes.

1. Introduction

Dielectric resonators are used in many electromagnetic devices such as all-dielectric metasurfaces and dielectric resonator antennas (DRA) [1]-[3]. At optical frequencies as well as higher microwave and millimeter wave frequencies, these resonators present a route around the ohmic losses in metallic resonators. Yet, many dielectric resonator structures have also been demonstrated at lower microwave frequencies, where the variety of high-permittivity dielectrics is greater. In fact, several water-based devices have been demonstrated as liquid water is cheap and flexible and has a relatively high permittivity (~80) at lower microwave frequencies (< 3 GHz) [4]. One of the problems of using water is its losses, particularly at higher frequencies. A workaround is to combine water with e.g., metals or low-loss dielectrics; however, the latter are much more expensive. As an example, we want to highlight a hybrid metal-water resonator supporting a bound state in the continuum in a single resonator placed in a rectangular waveguide [4].

Presently, a new type of resonators, first demonstrated in [5], are studied. The resonators employed an impenetrable spherical impedances surface and were found to support highly subwavelength Mie-like resonances. Interestingly, the configuration in [5] has been investigated several times before that work, although for other purpose (like cloaking). A later work presented the study of a penetrable circular cylindrical impedance sheet divided into two parts with different impedances in [6], which supported more focused scattering. In both studies [5], [6], the media around the impedance sheets were that of free space.

The present work investigates the scattering properties of these reactive impedance sheets embedded into a high-permittivity dielectric. As resonances can be excited in both the dielectric medium and the impedance sheet, this may enable a simultaneous excitation of electric and magnetic resonances, potentially leading to more focused scattering. Such scattering properties are of high interest in metasurface transmitarrays, absorbers as well as DRAs. To design subwavelength scatterers with focused scattering, one of the generalized Kerker's condition must be satisfied [7]. Although many scatterers can satisfy one of Kerker's conditions, it is often away from resonance and thus the total scattering is low. In this work, we show that the conditions can be satisfied in a canonical structure at frequencies around maximum scattering. Specifically, we study the scattering of a linearly polarized plane wave incident on an infinitely long circular high-permittivity cylinder embedded with a coaxial impedance sheet. Our work is based on a semi-analytical approach as we provide the solution to the scattering coefficient, which we then use to numerically calculate the scattering efficiency and scattering front-to-back ratio. We consider an ideal configuration with no absorption losses and the impedance sheet being infinitely thin.

The paper is organized as follows: Section 2 introduces the configuration and presents the analytical results. Section 3

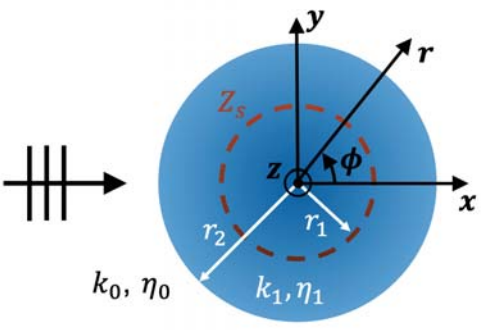

Figure 1. Sketch of the configuration.

presents the numerical results and discusses the realization and application of the proposed configurations, while Section 4 includes the summary and conclusion of the work. Throughout the paper, the time-factor exp(*jωt*), where ω is the angular frequency and t is the time, is assumed and suppressed.

2. Configuration and Theory

A sketch of the infinitely long circular cylinder is shown in Figure 1. A Cartesian coordinate system (x, y, z), and an associated cylindrical coordinate system (r, ϕ, z), is placed with their z-axes coincident with the cylinder axis. The cylinder consists of a dielectric medium with relative permittivity and radius r_2. A circular impedance sheet with the surface impedance $Z_s = R_s + jX_s$, with R_s (X_s) being the resistance (reactance), is embedded into the dielectric medium at radius r_1. The cylinder is situated in free-space and is illuminated by a linearly polarized plane wave propagating in the +x-direction. The cylinder will scatter the incident wave, and we have derived the solution to the scattering coefficients of the field outside the cylinder using the classical Lorentz-Mie analysis [8]. The impedance sheet makes the tangential magnetic fields discontinuous across its boundary, and thus the impedance boundary condition must be used at $r = r_1$. It is straightforward to show that the scattering coefficients can be expressed as

$$a_n^K = \frac{\xi_n^K J_n(k_0 r_2) - J_n'(k_0 r_2)}{H_n^{(2)\prime}(k_0 r_2) - \xi_n^K H_n^{(2)}(k_0 r_2)} \qquad (1),$$

with K = TE (transverse electric) or K = TM (transverse magnetic) denoting the polarization of the incident wave. Furthermore,

$$\xi_n^K = A^K \frac{J_n'(k_1 r_2) - \psi_n^K Y_n'(k_1 r_2)}{J_n(k_1 r_2) - \psi_n^K Y_n(k_1 r_2)} \qquad (2),$$

where $A^{\mathrm{TE}} = (\eta_1/\eta_0)^2 A^{\mathrm{TM}} = \eta_1/\eta_0$ and

$$\psi_n^{\mathrm{TE}} = \frac{J_n'(k_1 r_1)^2}{J_n'(k_1 r_1) Y_n'(k_1 r_1) + \frac{j2Z_s}{\pi \eta_1 k_1 r_1}} \qquad (3),$$

To obtain the expression for ψ_n^{TM}, the primes in the Bessel and Hankel functions in Eq. (3) are simply removed. Here, $k_0 = 2\pi/\lambda_0 = \omega\sqrt{\varepsilon_0 \mu_0}$ ($k_1 = k_0\sqrt{\varepsilon_r}$) and $\eta_0 = \sqrt{\mu_0/\varepsilon_0}$ ($\eta_1 = \eta_0/\sqrt{\varepsilon_r}$) are the wave number and intrinsic impedance of the (dielectric) free-space medium, respectively, with λ_0, ε_0 and μ_0 being the free-space wavelength, permittivity and permeability, respectively. Furthermore, J_n and Y_n are Bessel functions of the first and second kind, respectively, and $H_n^{(2)}$ is the nth order Hankel function of the second kind. The prime $'$ denotes the derivative with respect to the entire argument. To evaluate the scattering characteristics, we use scattering efficiency [8]

$$Q_{\mathrm{sca}}^K = \frac{2}{k_0 r_{\max}} \left(|a_0^K|^2 + 2 \sum_{n=1}^{\infty} |a_n^K|^2 \right) \qquad (4),$$

where $r_{\max}$ is the largest radius of the cylinder. Furthermore, we use the scattering front-to-back ratio (FBR) to evaluate the forward (+x-direction) vs. backward (–x-direction) scattering, and this is given by

$$\mathrm{FBR}^K = \frac{|a_0 + 2\sum_{n=1}^{\infty} a_n^K|^2}{|a_0 + 2\sum_{n=1}^{\infty} (-1)^n a_n^K|^2} \qquad (5).$$

3. Results

Presently, we consider the surface impedance to be lossless (R_s = 0), and thus $Z_s = jX_s$. When $X_s < 0$ ($X_s > 0$), the impedance sheet is capacitive (inductive). In the case of X_s = 0, the impedance sheet is a perfect electric conductor (PEC), and for $X_s \to \infty$, the impedance sheet vanishes as the tangential magnetic fields are continuous again. First, we consider the dielectric medium to be that of free space, i.e., ε_r = 1, and Eq. (1) reduces to

$$a_n^{\mathrm{TE}} = \frac{J_n'(k_0 r_1)^2}{J_n'(k_0 r_1) H_n^{(2)\prime}(k_0 r_1) + \frac{j2Z_s}{\pi \eta_0 k_0 r_1}} \qquad (6),$$

for TE incidence, whereas for TM incidence the primes in the Bessel and Hankel functions are simply removed in Eq. (6). For electrically small cylinders ($k_0 r_1 \ll 1$), we find the following conditions for maximum scattering: $a_0^{\mathrm{TM}} = 1$ for $Z_s = j\eta_0 k_0 r_1 \ln(1.781 k_0 r_1/2)$ and $a_0^{\mathrm{TE}} = a_1^{\mathrm{TM}} = 1$ for $Z_s = -j\eta_0\, k_0 r_1/2$. These peaks in scattering are caused by the currents induced on the impedance sheet. In the case of TM (TE) incidence, the modes n = 0 and n = 1 correspond to electric (magnetic) and magnetic (electric) dipole resonances, respectively. Note that these resonances are excited with a capacitive impedance sheet, which was also needed with a spherical impedance sheet in [5]. As $k_0 r_1 \to 0$, $Z_s \to 0$ and thus, no resonances are excited, since the cylinder is a simple PEC.

In Figure 2, we show the scattering efficiency (in dB) for a TE plane wave incidence on cylinders of various radii and three surface impedances ($Z_s = -j5$, $Z_s = 0$ and $Z_s = j5$). The radii are given in fractions of the free-space wavelength, and thus the results are valid at any frequency as long as the material values are retained. We choose ε_r = 80, similar to that of water at microwave frequencies [4]. However,

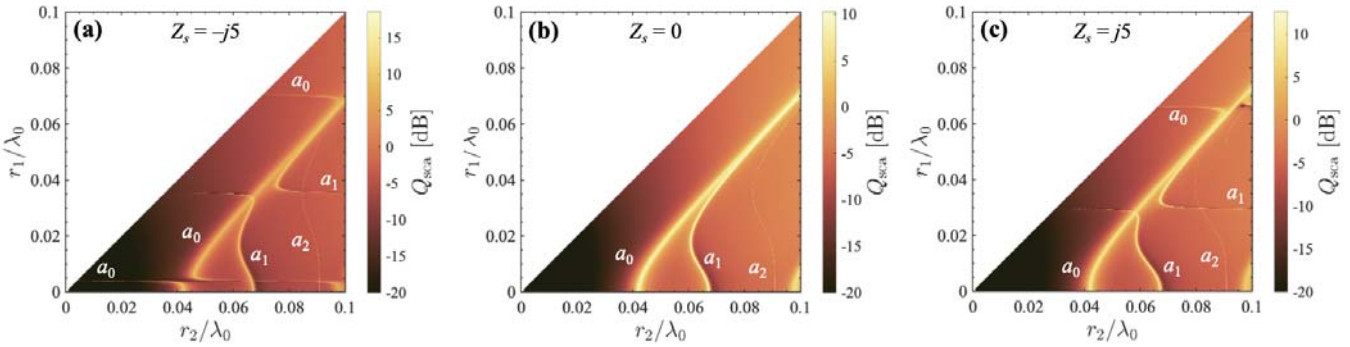

Figure 2. Scattering efficiency (colors) in logarithmic scale (dB) as a function of the radii of a dielectric cylinder (ε_r = 80) embedded with impedance sheet of **(a)** $Z_s = -j5$, **(b)** $Z_s = 0$ and **(c)** $Z_s = j5$. The coefficients a_n denote the resonance type causing the peaks in scattering with n = 1, 2 and 3 being the magnetic dipole, electric dipole and magnetic quadrupole, respectively.

Mie resonances can be excited in materials with even lower permittivities.

When $Z_s = 0$, the fields are zero in the inner dielectric layer ($r < r_1$), and thus the peaks in scattering we find in Figure 2(b) are due to Mie resonances excited in the outer dielectric layer. For very small r_1, we have the response of a regular dielectric cylinder, whereas for larger r_1 the magnetic (a_0) and electric (a_1) dipole resonances mix. Similarly, the magnetic quadrupole progress towards the dipoles as r_1 increases. Interestingly, these results show that introducing a conducting core inside the cylinder provides a mean to coincide the magnetic and electric resonances, and thus to satisfy one of Kerker's conditions.

Figure 2(a) and (c) show the scattering efficiency for a cylinder with $Z_s = -j5$ and $Z_s = j5$, respectively. The reactive impedance sheets introduce Mie-like resonances, which mainly depend on the radius of the impedance sheet. As predicted by Eq. (6), the capacitive surface impedance provides a magnetic dipole resonance for very small sizes. Interestingly, we observe that the resonance size is $r_1 \approx 0.004\lambda_0 \approx j2Z_s/(\eta_0 k_0)$, i.e roughly the same as when ε_r = 1, and thus the dielectric medium has only little influence on the resonance size. As r_2 increases, resonances will also be excited in the outer dielectric layer, thus enabling paired resonance excitations (magnetic-magnetic and magnetic-electric). However, excitation of the same resonance type, e.g. the magnetic dipole (n = 0), causes coupling resulting in low scattering efficiency. The mode splits into two branches in Figure 2(a) as it can only be excited in either the inner or the outer dielectric layer, and not in both at the same time. This stems from the negative surface reactance not just causing a discontinuity in the tangential magnetic field, but also reverse the orientation of the field. Thus, the volume displacement currents will be oppositely directed in the two layers. Similar observation is made for the electric dipole (n = 1).

The results for the inductive impedance sheet in Figure 2(c) are very similar, but there is no magnetic dipole resonance excited at small radii. Furthermore, the crossing of the magnetic and electric dipole resonances occurs at smaller radii compared to the capacitive impedance sheet.

The simultaneous excitations of magnetic and electric resonances are further investigated in Figure 3, where the frequency response of the scattering efficiency and FBR is shown. The radii are given in the figure caption and $Z_s = -j5$. In Figure 3(a), we show the simultaneous excitation of a magnetic dipole (inner layer) and an electric dipole (outer layer). As previous stated, this can result in a focusing of the scattering, which in this case is in the $\pm x$-direction depending on the phases of the dipoles. In Figure 3(a), we find a peak in the FBR (10 dB) very close to a peak in the scattering efficiency (11 dB), thus showing that Kerker's condition is roughly satisfied, albeit not perfectly. The magnetic (colors) and electric (arrows) fields in the cross section of the cylinder are shown at the frequency of the FBR peak in an inset in Figure 3(a). A large magnetic field is excited in the inner layer corresponding to a magnetic dipole. In the outer layer, a strong $-y$-directed electric field is found at the center of the cylinder corresponding to an electric dipole in a single-layered cylinder under TE-incidence. There is a second FBR offset from the peak in the scattering efficiency. Here, one of Kerker's conditions is satisfied, however, being away from the resonances, the scattering efficiency is low (–4 dB).

In Figure 3(b), we also have simultaneous excitations of magnetic and electric dipole resonances, but being switched to opposite layers. Similarly, we find a peak in the FBR (10 dB) and scattering efficiency (12 dB). Investigating the fields in the inset included in Figure 3(b), we clearly see that an electric (magnetic) dipole is excited in the inner (outer) layer. At last, we have also included the results for simultaneous excitation of a magnetic quadrupole (n = 2) and electric dipole in Figure 3(c). The electric dipole (magnetic quadrupole) is excited in the inner (outer) layer, which can be seen by the fields included as an inset in Figure 3(c). This combination of a higher order mode (n > 1) and a dipole resonance induced by the impedance sheet makes the peak scattering very narrow-banded. We observe that the peaks in the FBR (26 dB) and scattering efficiency (11 dB) overlap, and thus, the generalized Kerker's condition is satisfied.

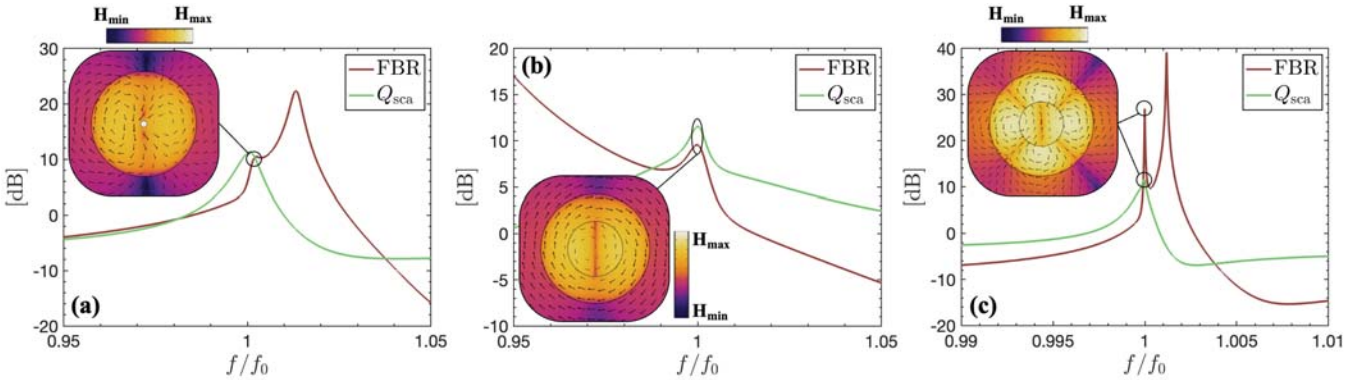

Figure 3. The scattering efficiency and FBR in logarithmic scale (dB) as functions of the normalized frequency f/f_0 with f_0 being the resonance frequency of the investigated resonances. **(a)** and **(b)** Results for the excitation of a magnetic dipole (a_0) and an electric (a_1) dipole is shown, whereas in **(c)**, we show the excitation of a magnetic quadrupole (a_2) and an electric dipole (a_1). The fixed parameters are K = TE, $Z_s = -j5$ and $\varepsilon_r = 80$, and r_1 (r_2) is approximately **(a)** $0.0041\lambda_0$ ($0.066\lambda_0$), **(b)** $0.034\lambda_0$ ($0.067\lambda_0$) and **(c)** $0.036\lambda_0$ ($0.085\lambda_0$). The insets show the magnetic (electric) fields as colors (arrows) in logarithmic scale in the xy-plane.

The presented results are for an ideal case, where losses are absent, and the surface impedance is smooth. Any losses, coming from the dielectric medium and/or the impedance sheet, will cause a lowering in the resonance intensity, and thus a reduction in the scattering efficiency. In the example of water as the dielectric medium with $\varepsilon_r \approx 80 - j1.3$ (f = 300 MHz and temperature is 20 °C), the magnetic quadrupole is a dark mode with no noticeable scattering. However, the scattering caused by the excitation of magnetic and electric dipoles is still significant. Despite the high losses, water presents a great and easy way to realize the presently proposed resonators and validate their scattering characteristics, since water is very flexible with its liquid form and adjustable permittivity. In fact, this hybrid combination of water and metallic impedance sheets may be a route around the low efficiency of water-based devices and extend their use beyond absorbers, and will be a subject of future studies.

4. Conclusions

In this work, we studied the resonant scattering of a high-permittivity infinitely long, circular cylinder embedded with an impedance sheet. We presented the analytical solution to the scattering coefficients, which we used to evaluate the scattering efficiency. First, we showed that highly subwavelength Mie-like resonances can be excited in the case of the dielectric being free space. Second, we showed the results for a lossless cylinder with the relative permittivity of 80 for TE plane wave illumination. We calculated the scattering efficiency for various cylinder and impedance sheet sizes for three surface impedance values ($-j5$, 0 and $+j5$). The results showed several designs supporting simultaneous excitation of electric and magnetic resonances. We made a deeper analysis of these simultaneous resonances for the case of a negative (capacitive) surface impedance exhibiting good front-to-back scattering ratio together with excellent scattering efficiency. At last, we discussed the realization of these resonators by using water as the dielectric medium with its high permittivity and flexibility.

We believe that these resonators have potential use in metasurface transmitarrays and Huygens source antennas as well as graphene nanotubes.

References

[1] S. Jahani and Z. Jacob, "All-dielectric metamaterials," *Nature Nanotechnology*, vol. 11, no. 1, pp. 23–36, Jan. 2016, doi: 10.1038/nnano.2015.304.

[2] S. B. Glybovski, S. A. Tretyakov, P. A. Belov, Y. S. Kivshar, and C. R. Simovski, "Metasurfaces: From microwaves to visible," *Physics Reports*, vol. 634, pp. 1–72, May 2016, doi: 10.1016/j.physrep.2016.04.004.

[3] A. Petosa and A. Ittipiboon, "Dielectric resonator antennas: A historical review and the current state of the art," *IEEE Antennas and Propagation Magazine*, vol. 52, no. 5, pp. 91–116, Oct. 2010, doi: 10.1109/MAP.2010.5687510.

[4] R. E. Jacobsen, S. Arslanagić, and A. V. Lavrinenko, "Water-based devices for advanced control of electromagnetic waves," *Applied Physics Reviews*, vol. 8, no. 4, p. 041304, Oct. 2021, doi: 10.1063/5.0061648.

[5] A. Sihvola, D. C. Tzarouchis, P. Ylä-Oijala, H. Wallén, and B. Kong, "Resonances in small scatterers with impedance boundary," *Physical Review B*, vol. 98, no. 23, p. 235417, Dec. 2018, doi: 10.1103/PhysRevB.98.235417.

[6] C. Valagiannopoulos and A. Sihvola, "Limits for scattering resonances in azimuthally inhomogeneous nanotubes," *Journal of Optics*, vol. 23, no. 12, p. 125609, Nov. 2021, doi: 10.1088/2040-8986/AC3961.

[7] R. Alaee, R. Filter, D. Lehr, F. Lederer, and C. Rockstuhl, "A generalized Kerker condition for highly directive nanoantennas," *Optics Letters*, vol. 40, no. 11, p. 2645, Jun. 2015, doi: 10.1364/ol.40.002645.

[8] C. F. Bohren and D. R. Huffman, *Absorption and scattering of light by small particles*, 1st ed. New York: John Wiley & Sons: Hoboken, 1983.